Removal of antibiotics by adsorption and catalytic ozonation using magnetic activated carbons prepared from Sargassum sp.

Marckens Francoeur, Christelle Yacou, Eddy Petit, Dominique Granier, Valérie Flaud, Sarra Gaspard, Stephan Brosillon, André Ayral

Removal of antibiotics by adsorption and catalytic ozonation using magnetic activated carbons prepared from *Sargassum sp.*

Marckens Francoeur[a,b,*], Christelle Yacou[a], Eddy Petit[c], Dominique Granier[d], Valérie Flaud [d], Sarra Gaspard [a], Stephan Brosillon[c], André Ayral[c]

[a] Laboratory COVACHIM-M2E, EA 3592 Université des Antilles, BP 250, 97157 Pointe-à-Pitre, Cedex, Guadeloupe

[b]URE, Université d'État d'Haïti, Port-au-Prince, Haïti

[c] Institut Européen des Membranes, IEM – UMR 5635, ENSCM, CNRS, Univ Montpellier, Place Eugène Bataillon, Montpellier, France

[d] Institut Charles Gerhardt Montpellier, ICGM – UMR 5253, CNRS, ENSCM, Univ Montpellier, 1919 route de Mende, Montpellier, France

Abstract

This study was carried out to determine the best conditions for the preparation of magnetic activated carbons (mACs) from *Sargassum sp.* as both adsorbents and catalytic supports. Coupling of adsorption and catalytic ozonation for removal and degradation of antibiotics was implemented for several cycles of use in order to assess the efficiency and the stability of these mACs. The mAC prepared by the post-impregnation method (activated carbon with *Sargassum sp.* + $FeCl_2.4H_2O$ pyrolyzed at 200 °C for 120 minutes) showed better adsorption capacity of a mixed solution of antibiotics (95.3, 48.3, 13.4 mg g^{-1} for tetracycline (Tc), penicillin (Pen) and erythromycin (Ery) respectively after 3 cycles of use) than the mAC prepared by

* Corresponding authors: *Marckens.Francoeur@etu.univ-antilles.fr*

the pre-impregnation method (*Sargassum sp.* + $FeCl_2.4H_2O$ pyrolyzed at 664 °C for 65 minutes). Whereas the evaluation of the degradation under ozone after mAC saturation by adsorption showed a better degradation after 3 cycles of reuse higher than 96% for Ery, and higher than 99% for Tc and Pen for the mAC prepared by the pre-impregnation method. Their physicochemical properties were characterized by different techniques, in particular X ray diffraction (XRD), Fourier transform infrared spectroscopy (FTIR), X-ray photoelectron spectrometry (XPS), analysis of the surface acid-base groups by Boehm method, pore analysis and specific surface area measurement (using the Brunauer–Emmett–Teller method) by nitrogen adsorption, scanning electron microscopy (SEM) and thermogravimetric analysis (TGA). The use of *Sargassum sp.* is therefore promising for the preparation of efficient bio-sourced mCAs for the removal of organic pollutants from polluted waters.

Keywords: *Sargassum sp.*, magnetic activated carbon, adsorption, catalytic ozonation, antibiotics

1. Introduction

Issues related to the presence of emerging micropollutants in the environment, such as antibiotics, continue to raise concerns. These molecules represent a danger for both humans and wildlife, due to their relatively low degree of biodegradability and, above all, their possible effect on increasing the resistance of bacteria once released into the environment [1–4]. Various strategies including separation [5], adsorption [6] and advanced oxidation [7–11] processes have been used to remove antibiotics from wastewater.

In that regard, activated carbon (ACs) are widely used for adsorption of many pollutants due to their large specific surface area and simple production methods [12]. However, they only concentrate the contaminants without ultimately removing them [13] and their regeneration is an obstacle to their large-scale application [14]. Advanced oxidation processes can convert antibiotic molecules into simple oxidized compounds or achieve complete mineralization [13,15]. To increase the efficiency of pollutants treatment and to reduce operational costs, the combination of several processes is currently being considered [8,16,17]. A promising combination is adsorption on ACs coupled with an ozonation operation (both together and after adsorption). However, the degradation of the AC surface during ozonation limits its long-term use [3,17–20]. To this end, the idea of using magnetic ACs (mACs) acting as catalysts in ozonation processes is herein considered. Such catalysts, especially those made from inexpensive precursors, can be easily separated from the treated water by applying an external magnetic field, thus proving to be economical and more environmentally friendly [8,21].

For a decade now, *Sargassum sp.* algae have caused dramatic inundation of North Atlantic and Caribbean seashores, hence becoming increasingly problematic. The amount of seaweed washing up on these beaches contributes to economic disruptions from tourism, aquaculture, traditional fishering and more recently has raised environmental concerns. To minimize these negative impacts, one of the proposed solutions is to collect the seaweed within 48 h to consider potential valorization. Indeed, due to those expansive beds they form, they are considered as the largest producers of biomass, growing to over a meter tall. *Sargassum sp.* has thus been used for its alginate extraction, as biosorbent material and more recently successfully converted into activated carbons (ACs) [22–24].

This work focuses on developing magnetic activated carbons (mACs) as ozonation catalysts derived from renewable precursor, *Sargassum sp.* algae. The resulting mACs were synthetized via two simple methods: post impregnation and pre-impregnation of iron precursor followed by an appropriate thermal treatment. Those synthesis routes were explored to seek optimal stability of the material during ozonation in tandem with their ability for magnetic separation. Prior catalytic ozonation, isothermal adsorption measurements on mACs were performed with three typical pollutants tetracycline (Tc), caffeine (Caf) and methylene blue (MB), to identify the best mAC candidate in term of adsorption efficiency. Then, the catalytic activity of mAC in the degradation of para-chlorobenzoic acid (pCBA) (a probe molecule) was evaluated in order to determine the catalyst efficiency in generating hydroxyl radicals •OH. Finally, the degradation of a mixture of antibiotics (tetracycline (Tc) + penicillin (Pen) + erythromycin (Ery)) under ozone after saturation of mACs, was investigated. Although the use of this technology in treating wastewaters has been documented to a great extent [25,26], the research on the removal of mixture of antibiotics by this type of immobilized biomass is still new and research efforts in this direction are considered as vital.

2. Materials and methods

2.1 Chemical products

Tetracycline (Tc, purity ≥ 98%, Lot. 097M4852V), penicillin G sodium salt (Pen G purity ≥ 96%, Lot. 039M4795V), para chlorobenzoic acid (pCBA, purity ≥ 99%, Lot. 135585), caffeine (Caf, purity ≥ 98.5%, Lot. 021M0092V) were purchased from Sigma-Aldrich. Pure methylene blue (MB, Lot. 310 95-7) was purchased from RAL Reagents. Erythromycin (Ery, purity ≥ 98%, Lot. HP6IA-PI) was purchased from Tokyo Chemical Industry.

Raw *Sargassum sp.* was collected in the Caribbean area (Guadeloupe French west-indies), washed, sun-dried, grounded and finally sieved to particles size between 0.4 mm to 1mm. The alga collection was carried out in March 2021. All other chemical reagents in the study H_3PO_4 (85 wt%), NaOH, HCl, $FeCl_3.6H_2O$, $FeCl_2.4H_2O$ were of analytical grade. Stock solutions were prepared separately by dissolving an appropriate amount of the powdered compounds in ultrapure distilled water (15 MΩ).

2.2 Preparation of mACs derived from *Sargassum sp.*

Two different procedures were used for the preparation of the mACs, which consist of the post- or pre-impregnation of iron precursors ($FeCl_3.6H_2O$ and $FeCl_2.4H_2O$). The simplified flowchart of the synthesis procedure is shown in **Fig. 1**. For comparison purpose, unsupported iron oxide catalyst and pure activated carbon were also prepared (herein referred to as Fe_xO_y and AC_OP, respectively). Details of their synthesis are given in **SI 1**.

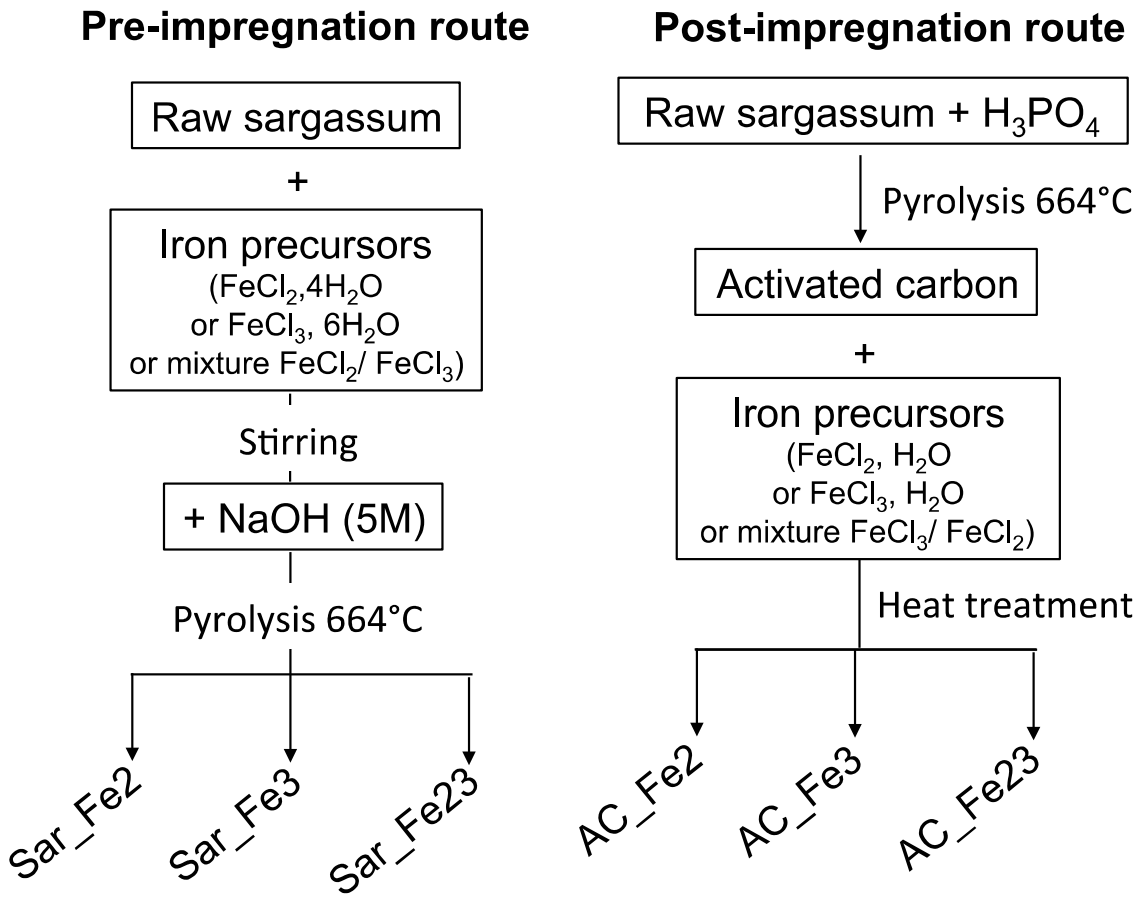

Fig. 1 Flow chart of the mACs synthesis.

Details about synthesis process of pure activated carbon (label AC_OP) are provided in previous study [12].

2.3 Adsorption capacity measurements of ACs

Adsorption isotherms of methylene blue (MB), tetracycline (Tc) and caffeine (Caf), were carried out at room temperature on the six prepared mACs as described on **Table S1**. Such experiments aim to identify the mAC with the highest adsorption capacity for each selected molecules. Calibration curves were obtained from UV-visible absorbance spectra of the solutions, recorded with a UviLine 9400

125 spectrophotometer. Absorbance maxima were identified at λ_{max} = 273, 358 and 663
126 nm for Caf, Tc and MB, respectively.
127 Experimental adsorption capacities, Q_e (mg g^{-1}), were calculated according to
128 equation (**1**)

$$Q_e = \frac{(C_0 - C_e).V}{W} \qquad (1)$$

129 where C_0 is the initial adsorbate concentration (mg L^{-1}), C_e, the adsorbate
130 concentration at equilibrium time (mg L^{-1}), V, the volume of the adsorbate solution
131 (L), and W, the mass of the adsorbent (g). Two models were used to fit the
132 experimental data by applying a non-linear regression, Langmuir model and
133 Freundlich model.
134

135 **2.4 Physicochemical characterization of ACs**

136 BET surface area and pore size distribution of the prepared solids (from the above
137 mentioned adsorption results), were evaluated via N_2 adsorption experiments at 77 K
138 using a Micromeritics analyzer (ASAP 2020 V4.04). Chemical surface groups of the
139 pristine and spent carbon materials (before and after ozonation exposure), were
140 determined by Fourier transform infrared spectroscopy (FT-IR spectrometer
141 equipped with an ATR accessory, Spectrum Two Perkin Elmer). Analysis of the
142 surface acid-base groups by Boehm method and the determination of the zero point
143 of charge (ZPC), were carried out following procedures described in a previous study
144 [23].
145 X-ray photon electron spectroscopy (XPS) of AC_OP before and after ozonation was
146 performed (ESCALAB 250 from Thermo Electron) with a monochromatic excitation
147 source, Al Kα line (1486.6 eV). The photoelectron spectra were calibrated in binding
148 energy with respect to the energy of the C=C component of C1s carbon at 284.4 eV.

149 Volatiles and ash (including iron oxides) contained in mACs were measured by
150 thermogravimetric analysis (TGA) in air at a heating rate of 10 °C min^{-1} from 25 to
151 1000 °C (TA Instruments Thermal Analysis DSC-TGA Standard).
152 Scanning electron microscopy (SEM) observations, combined with energy dispersive
153 X-ray (EDX) chemical analyses were performed with a HiVAC + VCD - Quanta 250
154 detector instrument (operated at 100 KeV). This aims to study the surface
155 morphology of samples followed by chemical mapping of various elements (Fe, O, P,
156 Ca, and S).
157 X-ray diffraction (XRD) analysis was done to identify the crystalline iron phases
158 present in the mACs. The diffractograms were obtained by scanning in 2θ between
159 23 and 96° with a step size of 0.04°, using a cobalt anode X-ray tube as the source
160 ($\lambda_{K\alpha\ Co}$ = 1.79 Å, power supply: 40 kV and 30 mA) and a Malvern Panalytical
161 Empyrean diffractometer.
162 Magnetic field applied to separate the mACs from the treated solution, was
163 measured, with a teslameter, in the air gap of an electromagnet as a function of
164 current intensity (4 A) and air gap distance (2 cm). It was equal to ~0.65 Tesla. The
165 mean separation time was also evaluated. The measurements were performed in a
166 1.5 cm diameter glass tube containing 500 mg of carbon and 5 mL of distilled water.
167 Finally, the measurement of the total leached iron concentration after each ozonation
168 cycle was measured by atomic absorption (AAnalyst 400 Perkin Elmer).
169

170 **2.5 Degradation of pCBA**

171 The decomposition of para chlorobenzoic acid (pCBA) using ozone O_3 on ACs was
172 firstly studied to define the characteristics of catalytic ozonation process. The pCBA
173 was chosen as a probe molecule for •OH monitoring as it has very low reactivity with

O_3 (constant rate $k_{O3/pCBA}$ = 0.15 M^{-1} s^{-1}), but reacts readily with •OH ($k_{.OH/pCBA}$ = 5 × 10^9 M^{-1} s^{-1}). In an ozonation system, the decomposition of the probe is an indirect measurement of the •OH concentration as a function of the time. Hence, calculating the term $\int[\bullet OH]dt$, defined by Elovitz and von Gunten [27], as the total amount of hydroxyl radicals to which a reference compound (pCBA) is exposed in the treated water, allows to quantify the exposure to hydroxyl radicals (equation (**2**)).

$$\int[\bullet OH]dt = \int \frac{\ln(\frac{\mathrm{pCBA_0}}{\mathrm{pCBA}})}{\mathrm{k}_{OH/pBCA} = 5.2\times10^9\ M^{-1}S^{-1}} \qquad \textbf{(2)}$$

Ozonation of a solution of pCBA (50 mg L^{-1}) with three ACs (AC_OP, AC_Fe3, and SAR_Fe2) derived from *Sargassum sp*. was carried out for 1 h. For this purpose 250 mL of pCBA solution was mixed with 150 mg of one of the ACs. The suspension was then stirred for 12 h to reach adsorption equilibrium. The ozonation experiments were carried out in a 500 mL batch reactor under 200 rpm stirring. The ozonated gas (concentration varying between 10 and 25 g Nm^{-3}) was introduced by bubbling, through a porous sinter at a flow rate of 15 L h^{-1} at 25 °C.

Sampling was carried out periodically the concentrations of pCBA (after equilibrium and ozonation treatment) were measured by UV-visible spectroscopy, after filtration of the supernatant through a 0.45 µm filter followed by 5 minutes of centrifugation at 9500 rpm. To evaluate the effect of AC reactivity after each ozonation, the mixture was centrifuged to remove the supernatant and added back to the 250 mL bottle of pCBA stock solution. Each measurement was triplicated.

2.6 Degradation of antibiotics

Mixed adsorption of the 3 molecules (Tc, Pen and Ery) on ACs, coupled with ozonation, was performed at pH 7. The adsorption was used (i) to concentrate

pollutants on the solid surface (i.e. near by the degradation sites), before ozonation [21], and (ii) to adsorb the by-products generated during ozonation step. Hence, adsorption measurement before ozonation allows a better assessment of the catalytic effect of ACs [28]. In addition, the reuse of ACs helps to estimate the degree of adsorption of the ozonation by-products upon the ACs surface. The pH was adjusted with a concentrated solution of HCl or NaOH after reaching adsorption equilibrium.

100 mL of each antibiotic solution (Pen, 100 mg L^{-1} + Ery, 100 mg L^{-1} + Tc, 250 mg L^{-1}) were mixed with 150 mg of the different ACs. pH was adjusted with a concentrated solution of HCl or NaOH after reaching adsorption equilibrium. The mixtures were stirred for 12 h at 25 °C in a water bath and were then placed in the ozonation pilot for 1 h (ozone concentration varying from 10 to 25 g Nm^{-3} at a flow rate of 15 L h^{-1}). Reuse for three cycles was carried out after removing the supernatant by centrifugation and the recovered AC was put back in contact with the same volume of the initial solutions. Sampling was carried out periodically quantification of antibiotics (after adsorption equilibrium and after ozonation), was performed by LC-MS chromatography after filtration of the supernatant with 0.45 µm filters and subsequent centrifugation for 5 minutes at 9500 rpm. Total leaching of iron into solution after each ozonation cycle was determined by atomic absorption (AAnalyst 400 Perkin Elmer).

3. Results and discussion

3.1 Adsorption isotherms

Adsorption experiments were conducted for all samples: pre-impregnated (SAR_Fe2, SAR_ Fe3 and SAR_Fe23), posted-impregnated (AC_Fe2, AC_ Fe3 and

AC_Fe23) and pure activated carbon (AC_OP) (**Fig. 2**). All capacities adsorption were obtained from Langmuir model with a R^2 between 0.90 to 0.98.

AC_Fe3 (obtained by the post-impregnation route), was identified as the best performing mAC sorbent for the three molecules. One the other hand, adsorption capacities on mAC were lower than those of AC_OP towards Tc and Caf, expect for MB where a maximum value of 310 mg^{-1} was reached with AC_Fe3. In addition, the same trend was observed in term of adsorption (i.e. order Tc > MB > Caf), suggesting similar properties of mACs.

Among the pre-impregnated samples, SAR_Fe2 shows the highest adsorption capacities for 2 of the 3 molecules Caf (142 mg g^{-1}) and MB (182 mg g^{-1}), while SAR_Fe23 shows the best uptake for Tc (242 mg g^{-1}) (**Fig. 2**). For comparison, Zhu et al [29] found a Tc adsorption capacity of 24.44 mg g^{-1} for hydrochar (coal obtained from hydrothermal carbonization), and Zhou et al [30] measured a capacity of more than 300 mg g^{-1} on magnetic coal prepared with wood, thus suggesting reasonable performance of the mAC samples. Based on these adsorption data, the following mAC samples SAR_Fe2 and AC_Fe3, were selected to proceed the ozonation degradation.

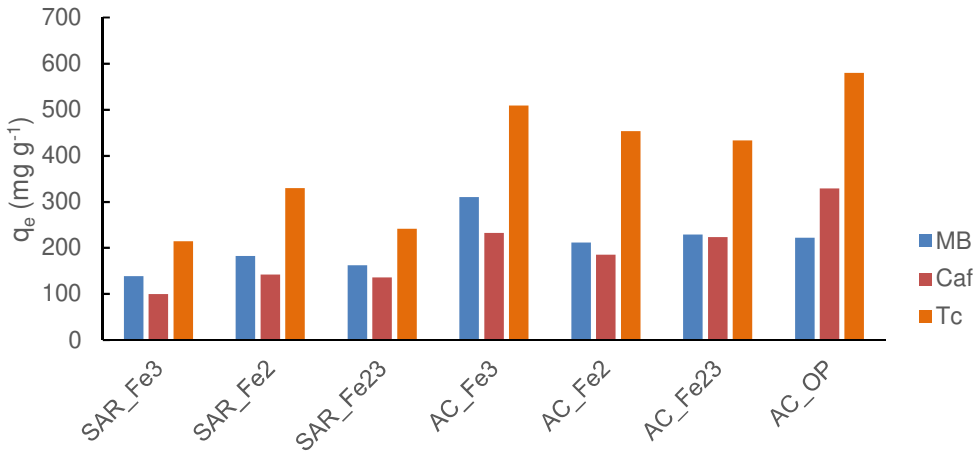

Fig. 2 Adsorption capacities of the different prepared ACs towards MB, Caf, and Tc.

3.2 Physicochemical characterization of ACs

Physicochemical properties of the synthetized samples were investigated via nitrogen sorption, SEM and TGA analysis. As depicted in **Table 1**, a decrease in surface area was observed between AC_OP (pure activated carbon) and AC_Fe3 (post-impregnated AC), but the latter exhibits a significantly higher specific surface area compare to SAR_Fe2 (**Table 1**). Besides, TGA and SEM/EDX results reveals lowest iron concentration in AC_Fe3 and the iron oxide particles formed in both mACs were uniformly distributed (**Fig. 3**). Further chemical analysis performed by EDX indicates the presence of common inorganic compounds such as C, Na, S, Ca, P, Mg, and O in all three ACs, in tandem with Fe in SAR_Fe2 and AC_Fe3 samples. Boehm titration results indicate that SAR_Fe2 has more basic than acidic surface clusters, in contrast to AC_Fe3 and AC_OP, which also agreed with ZPC values and FT-IR analyses.

These features are consistent with previous works showing that magnetization of biomass can reduce physicochemical properties of mACs such as BET surface area, pore volume, and acid-base groups [31]. Even though previous studies [31,32] reported promising magnetic separation when a high Fe content is used (i.e. mAC

261 with a C : Fe ratio close to 4), a too high magnetic phase content can affect
262 adsorption properties of mACs. With only 3.7% and 7.2% of iron oxide in our
263 samples AC_Fe3 and SAR_Fe2 respectively, a relatively fast average separation
264 time (337 s and 167 s, respectively), from the liquid phase was obtained, under a
265 magnetic field of ~0.65 T. Iron crystalline phase was determined by XRD
266 measurements (**Fig. 4a**) which indicate the presence of (i) Fe_3O_4 (diffraction peaks at
267 2θ = 35.08°; 41.39°; 50.46°; 67.24°; 74.14°), (ii) FeO (main peak at 2θ of 49.27°), (iii)
268 iron metal (main peak at 2θ = 52.36°) and (iv) Fe_xO_y [33]. Overall, magnetite Fe_3O_4
269 was the predominant Fe form contained in the mACs matrix, thereby confirming their
270 attractive magnetic properties.
271 To assess the stability of samples, FTIR measurements were carried out (i) before
272 and after ozonation treatment (ii) after 3 reuses of AC_OP and AC_Fe3 and
273 SAR_Fe2. The spectra displayed in (**Fig. 4b**), show absorbance bands at 1066 cm^{-1},
274 1558 cm^{-1}, 2952 cm^{-1}, 3526 cm^{-1} detected in 3 ACs, which were attributed to C-O, R-
275 COO, C-H, OH groups, respectively [34]. The band at 590 cm^{-1} assigned to metal,
276 confirms the presence of Fe_3O_4 in these ACs [35]. Interestingly, SAR_Fe2 exhibited
277 excellent surface bond stability compare to AC_Fe3 and AC_OP over the 5 tested
278 cycles with pCBA degradation. No clear changes were detected in its spectrum in
279 contrast with AC_OP and AC_Fe3, which show chemical surface modification. This
280 is also consistent with XPS analysis of the pure activate carbon AC_OP before and
281 after ozonation (**FigS. 1, FigS. 2**), showing a chemical modification of the coal
282 surface with the decrease of C=C and C-C groups, and an increase of C-O, C=O,
283 and O-C=O groups (Jans and Hoigné,1998).

284 **Table 1: Physicochemical characterization results of the different ACs.**

Sample	ZPC	Boehm (mmol g^{-1}) Acid	Basic	BET surface area (m^2 g^{-1})	Pore volume (cm^3 g^{-1})	TGA VM+FC[a] Ash (wt%)		EDX (at% Fe)
SAR_Fe2	8.5	2.77	6.34	248	V_{meso}: 0.11 V_{micro}: 0.02 V_{total}: 0.18	26	74	7.2
AC_Fe3	4.3	3.02	1.18	607	V_{meso}: 0.37 V_{micro}: 0.02 V_{total}: 0.54	57	43	3.7
AC_OP	5.8	4.60	2.19	929	V_{meso}: 0.78 V_{micro}: 0.02 V_{total}: 0.95	85	15	-
Fe_xO_y	-	-	-	5.4	V_{meso}: 0.02 V_{micro}: N/A V_{total}: 0.05	-	-	-

285 [a] VM + FC: volatile matter + fixed carbon in wt% without moisture

286

287

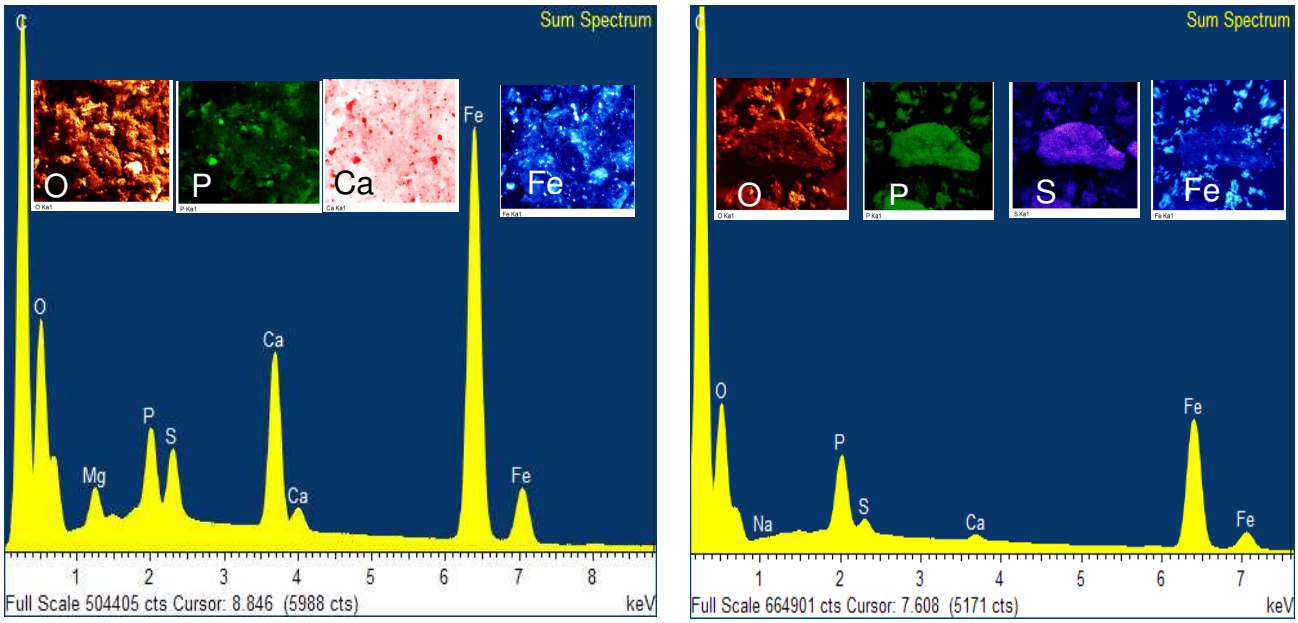

(a) (b)

288 **Fig. 3 SEM images and EDX analysis of (a) SAR_Fe2 and (b) AC_Fe3.**
289

290

291

292

293

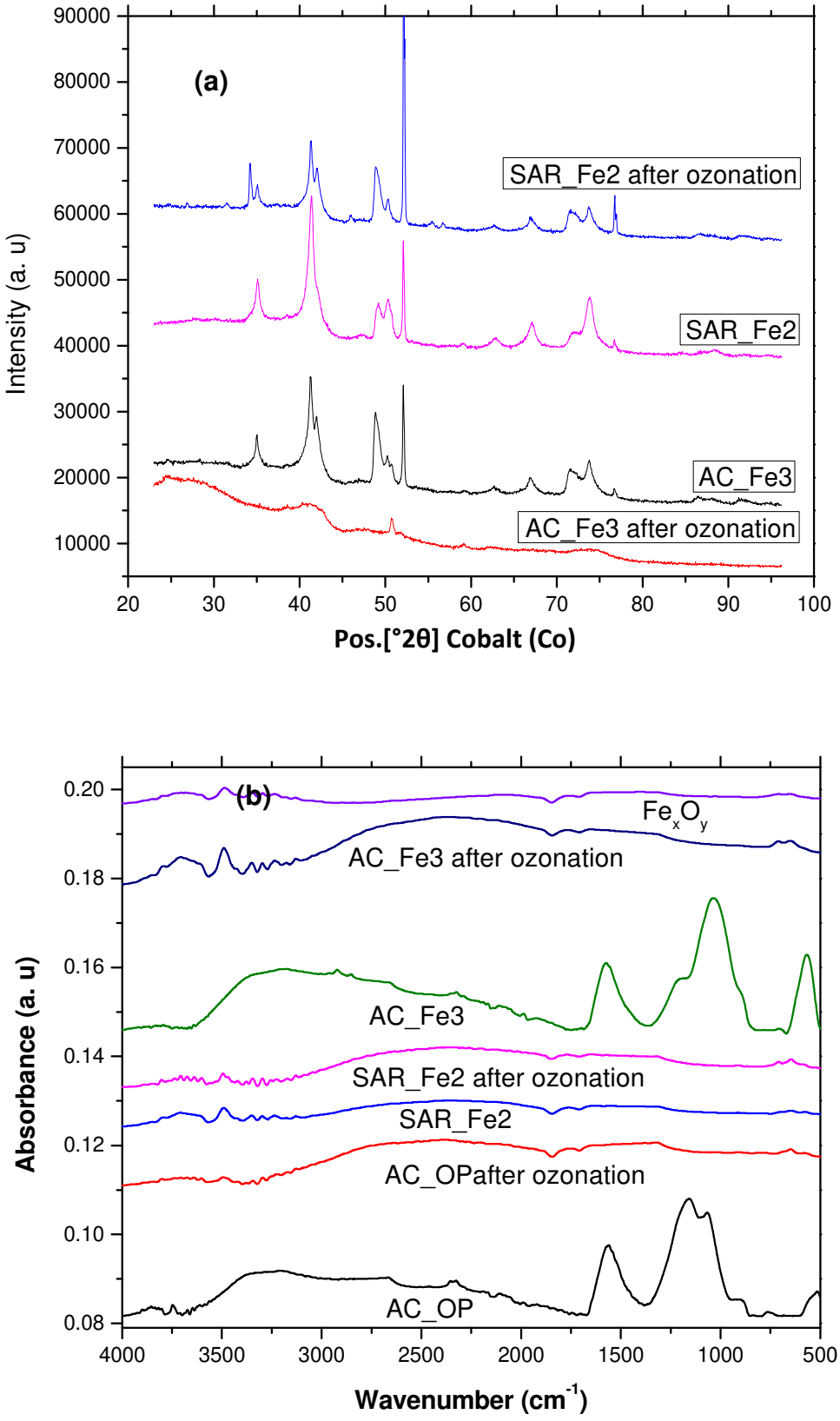

Fig. 4 (a) XRD patterns and (b) FTIR spectra of mACs before and after ozonation.

297 **3.3 Degradation of probe molecule pCBA**

298 The pCBA was chosen as a probe molecule due to its high reactivity with •OH
299 radicals [37]. If pCBA is well degraded, this implies that the solid has successfully
300 catalyzed the transformation of dissolved ozone into hydroxyl radicals (radical
301 pathway).

302 Analysis of the degradation of pCBA after ACs saturation (by adsorption of the
303 different ACs) shows that SAR_Fe2 exhibited excellent stability over the five tested
304 cycles, with high removal efficiency up to 97-98% (**Fig. 5**). Noteworthy, pH of the
305 mixtures varies from 5 (before ozonation) to 4.2 (after ozonation). As pCBA
306 ozonation was carried out at pH>3, such variation of pH was probably associated to
307 oxidation reactions taking place at the catalyst-solution interface and in bulk solution
308 as found by others (Park et al., 2004). In parallel, study of the variation of the O_3
309 concentration in the pilot showed that the degradation kinetics of pCBA nearby the
310 mAC surface, was very fast, (less than 10 min) [38].

311

312 Conversely, catalytic activities of AC_OP and AC_Fe3 were lower than of SAR_Fe2,
313 whilst declining quickly. For instance, for pure carbon (AC_OP), pCBA removal
314 decreased from 73% to nearly 20% over the three tested cycles. This severe
315 catalytic deactivation could be related to the fact that chemical surface bonds of
316 AC_OP (which allowed pCBA degradation over the 1st cycle) were denatured (**Fig**
317 **4b**), thereby hindering effective formation of •OH radicals [8,28]. Therefore,
318 adsorption capacity of AC_OP decreased significantly after each ozonation cycle.

319 Similar trend was observed for AC_Fe3 where ozone-induced degradation of pCBA
320 decreased after each cycle but remained higher than of degradation capacity of
321 AC_OP. With the presence of iron oxide in the AC_Fe3 matrix, its capacity to form

322 •OH radicals has therefore increased. Loss in adsorption capacity was also observed
323 in AC_Fe3, which thus contributed to the decline its catalytic effect, with a maximum
324 removal efficient of (56% of the initial pCBA concentration is observed).
325
326 Stability of samples was further assessed by performing (i) XRD measurements
327 before and after ozonation and (ii) atomic absorption analyses to determine the
328 amount of iron leached into solution after reaction. As shown in **Fig 4a**, diffraction
329 peaks (at 2θ = 35.08° and 67.27°) related to Fe_3O_4 in AC_Fe3, have significantly
330 decreased or disappeared after ozonation. This correlates well the values of iron of
331 0.33 and 1.46 mg L^{-1} found after the second and third cycles, respectively, indicating
332 slight dissolution of the iron impregnated in AC. One can note that such relatively low
333 levels of iron leaching are below the European Union Directive values of 2 mg L^{-1}. A
334 concentration of iron higher than 0.3 mg L^{-1} may increase the turbidity of the water
335 without being a proven health hazard [39].
336
337 As above mentioned, SAR_Fe2 seems to be the best catalytic candidate, with a
338 percentage removal greater than 92% after the first cycle which tends to increase
339 over the following cycles. Owing to the fact that pCBA adsorption on SAR_Fe2 was
340 measured to be less than 20%, this implies that all the removed pCBA was mainly
341 degraded during ozonation. As a comparison, pCBA degradation efficiency of 92.5%
342 was achieved by others through the addition of dissolved metal ion Fe^{2+} during
343 homogenenous catalytic ozonation [40].
344 After the third cycle, SAR_Fe2 was ozonated in 300 mL of ultrapure distilled water
345 for 3 h. XRD diffraction patterns of SAR_Fe after 5 cycles of use, shows enhanced
346 intensity of Fe_3O_4 peaks (at 2θ of 35.08°, 41.39°, 50.46°, 67.27°, and 74.14°) (**Fig.**

4**a**), while intensity of the main iron metal peak (at $2\theta = 49.27°$) tends to decrease. This could be explained by subsequent dissolutions of iron into solutions during ozonation, corresponding to iron leaching of 2.07, 5.26, and 5.37 mg L^{-1} after the first, third, and fifth cycle, respectively. This is in line with the results previously published by C.V Rekhate and J.K. Srivastava [8]. Overall SAR_Fe2 remains a stable mAC, exhibiting high activity for the production of •OH radicals during catalytic ozonation.

Finally, the exposure to hydroxyl radicals accordingly to the different ozonation experimental conditions was determined following equation (**2**). Results are listed in **Table 2** for AC_Fe3, AC_OP and SAR_Fe2 and were compared with other reported values. The results confirms that the catalytic ozonation with SAR_Fe2 shows a high generation of hydroxyl radicals.

3.4 Degradation of antibiotics

Kinetic data indicate the highest reactivity of antibiotics with hydroxyl radicals ($k_{OH} > 10^9$ M^{-1} s^{-1}) versus direct oxidation of molecular ozone ($k_{O3} > 10^5$ M^{-1} s^{-1}) [41]. Catalytic ozonation was carried out within the pH range of 7 – 3.6, since the measured pH of solutions varied between 3.68 and 6.26, after each cycle of ozonation. **Fig. 6** presents the degradation graphs of the three studied molecules (Tc, Pen G and Ery) over three cycles of ozonation, with an ozonation exposure time of 1h for each carbon material.

These results indicated that Tc adsorption capacity on AC_OP decreases up to 27% after the 2nd cycle of ozonation, whereas an increase in adsorption was observed for the mACs (from 37% to 58% for SAR_Fe2, and from 78% to 82% for AC_Fe3). After

372 the three cycles, optimal Tc degradation value of ~99% was achieved for all carbon
373 samples. In comparison, Kakavandi et al. [42] observed a loss of efficiency after 180
374 minutes of mAC use for Tc degradation, and complete Tc removal was obtained
375 beyond 60 minutes when the ozonation/ mAC process was coupled with other
376 chemical oxidants. In addition, Lu et al. [43] demonstrated that when using a
377 bifunctional catalyst, in a coupled ozonation/photocatalysis process, a decrease of
378 88% in total organic carbon (TOC) was achieved within 80 minutes for a Tc solution.
379 For Pen G, opposite trend was observed on AC_OP where adsorption capacity
380 values increased very significantly from 4% to 69%. Enhancement in Pen G
381 adsorption was also obtained on the mACs (24% and 40% for SAR_Fe2 and
382 AC_Fe3, respectively). This strongly suggests that the affinity of Pen G has thus
383 increased over the three cycles leading to a better removal (> 99%) of the molecule
384 during ozonation. This increase in affinity can be associated with the appearance of
385 FT-IR bands at 3526 cm^{-1} for AC_Fe3 and AC_OP, corresponding to the elongation
386 vibrations of OH surface groups [19].
387 The optimization study by Hekmatshoar et al [44] previously showed that the
388 efficiency of the simple adsorption process on AC, the simple ozonation process,
389 and the catalytic ozonation process with AC were 11%, 33%, and 85%, respectively,
390 when removing Pen G at pH 10.
391 AC_OP has a very good affinity for Ery and its adsorption capacity increases by 20%
392 after the ozonation cycles. Very low adsorption is observed for SAR_Fe2 against a
393 clear increase (47%) in the adsorption capacity of AC_Fe3. The removal of Ery is not
394 complete after the three ozonation cycles on the different carbons. A 93 % removal
395 is observed on SAR_Fe2, 97% on AC_OP and 98% on AC_Fe3. For comparison,
396 Danalıoğlu et al [45] had measured, for a mAC, an adsorption capacity of 178.6 mg

397 g^{-1}, and desorption efficiency of Ery lower than 20% after more than 5 hours for
398 different solutions. Degradation of Ery after three cycles on multi-walled carbon
399 nanotubes in the presence of ozone leads to a TOC/TOC_0 ratio higher than 0.7 [46].
400 The study by Alameddine et al [47] showed that the combination of AC and O_3 was
401 very efficient for the degradation of micropollutants including antibiotics. However,
402 the prepared AC could neither degrade nor adsorb pollutants after a first use.
403
404
405

406

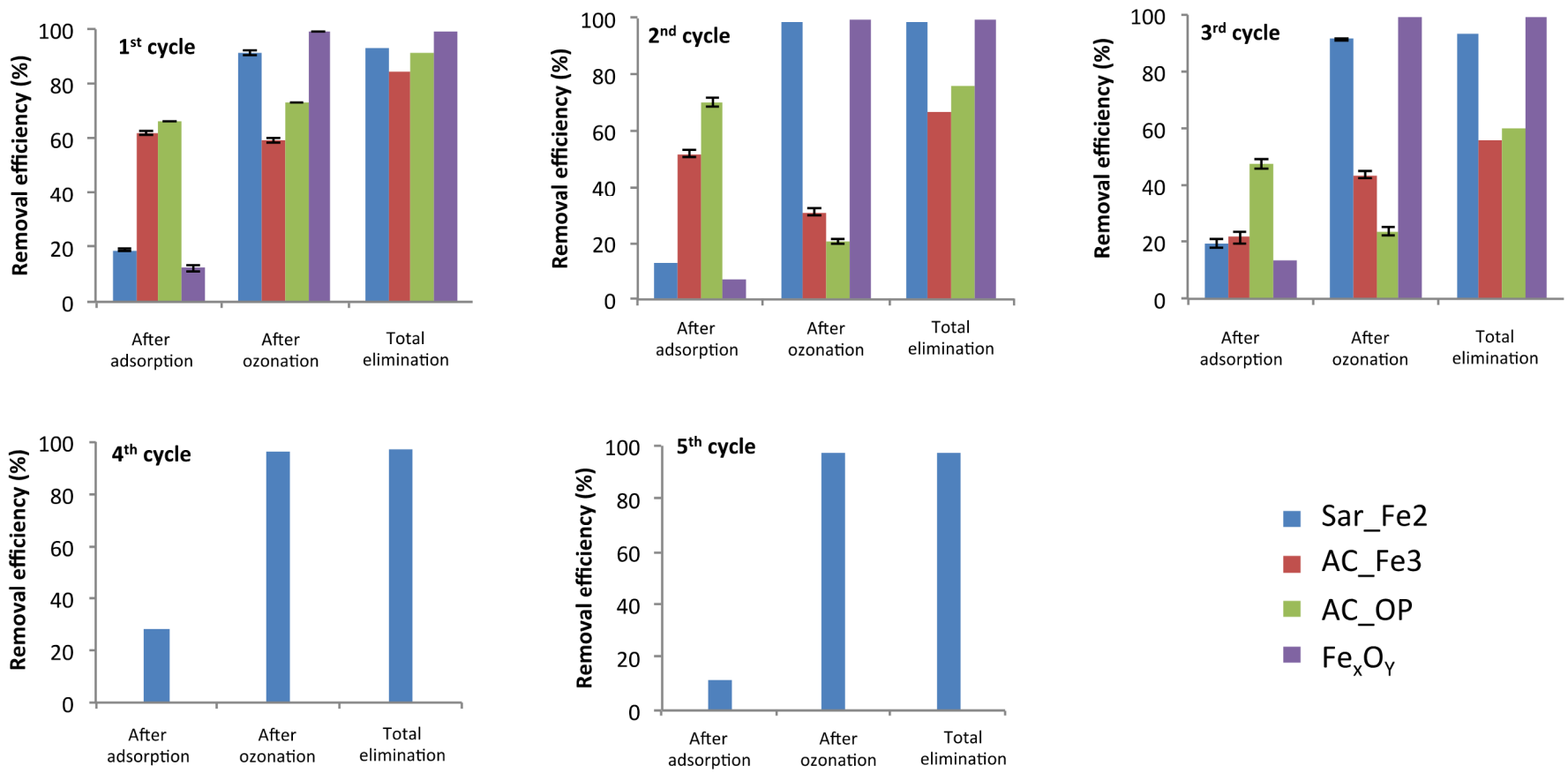

407

408 **Fig. 5 Catalytic effect of ACs and Fe_xO_y on the degradation of pCBA in the presence of ozone, after several cycles of use**
409 **(concentration between 10 and 25 g Nm^{-3}, total duration : 1 h).**

Table 2. Production of hydroxyl radicals for different catalytic ozonation.

Catalytic ozonation	mol^{-1} s^{-1}	References
Ozone + nano zinc oxide	1.7624×10^{-11}	[38]
Alkaline catalytic ozonation	3.5867×10^{-10}	[45]
Ozone + SAR_Fe2	7.10×10^{-10}	This work
Ozone + AC_OP	1.77×10^{-10}	This work
Ozone + AC_Fe3	1.57×10^{-10}	This work

4. Conclusion

Magnetic activated carbons based on the biomass *Sargassum sp.* were prepared to allow magnetic separation and to be used as catalytic ozonation supports for the removal of tetracycline, penicillin, and erythromycin from water. Our work showed that the different materials selected (AC_Fe3, AC_OP, and SAR_Fe2) were effective in producing hydroxyl radicals after three cycles of use. Stability of SAR_Fe2 is demonstrated after more than five cycles of use, with a pCBA degradation performance of more than 92% during ozonation.

The advanced oxidation process based on ozonation coupled with ACs used as catalytic support showed its efficiency in removing pollutants, with a removal rate of more than 96% for Ery, and more than 99% for Pen and Tc, after three cycles of use. These results, therefore, provide new possibilities for the use of *Sargassum sp.* algae for the removal of pollutants from wastewater. However, certain aspects such as the kinetics and mechanisms of pollutant degradation, the performance of AC in real wastewater, and the optimization of the ozone utilization rate must be deepened order to conclude on the technological applicability of this hybrid process, before promoting a large-scale implementation of these new bio-sourced and multifunctional activated carbons.

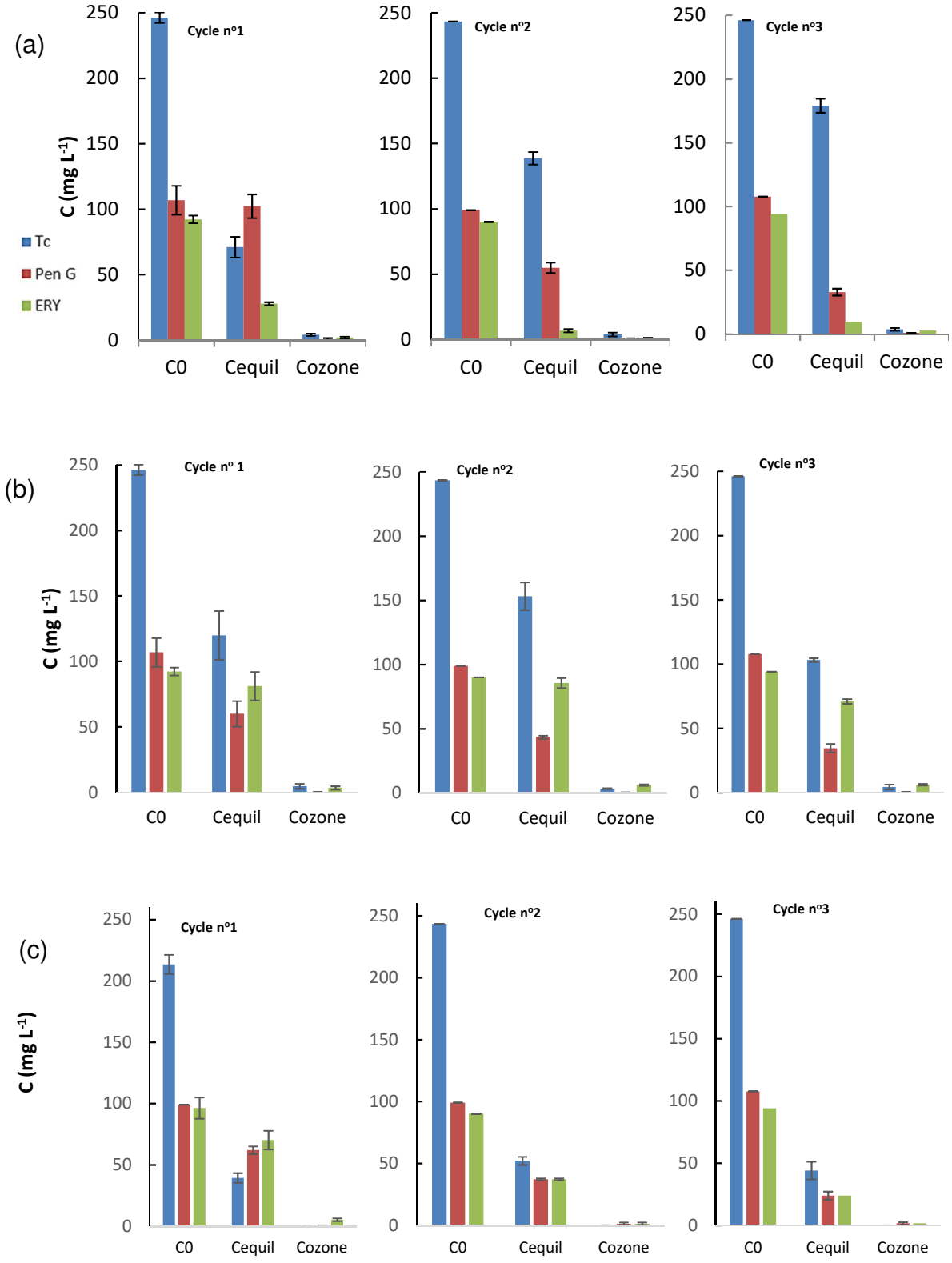

Fig. 6 Solution concentration of Tc, Pen and Ery at pH 7 after the different steps: Initial (C_0) / Adsorption equilibrium (C_{equil}) / Catalytic ozonation (C_{ozone}), t = 1 h for each AC after 3 cycles: (a) AC_OP; (b) SAR_Fe2; (c) AC_Fe3.

E-supplementary data of this work can be found in online version of the paper

Acknowledgments

The authors wish to thank Nathalie Masquelez, Martin Drobek, Loubna Karfan Atfane, Jim Cartier from IEM for their technical support in carrying out thermogravimetric analysis, nitrogen adsorption and ozonation reactor implementation, respectively. The financial support for this work was mainly provided by the Cooperation Service of the French Embassy in Haïti and The Université Publique du Sud-Est à Jacmel.

Credit authorship contribution statement

Marckens Francoeur: Data curation, Methodology, Formal analysis, Validation, Visualization, Writing - original draft. Eddy Petit, Dominique Granier, Valérie Flaud: Data curation, Formal analysis. Sarra Gaspard, Stephan Brosillon, Christelle Yacou: review & editing and André Ayral review & editing, Supervision.

References

[1] F. Gagné, C. Blaise, C. André, Occurrence of pharmaceutical products in a municipal effluent and toxicity to rainbow trout (Oncorhynchus mykiss) hepatocytes, Ecotoxicol Environ Saf. 64 (2006) 329–336. https://doi.org/10.1016/j.ecoenv.2005.04.004.

[2] Q. Yang, Y. Gao, J. Ke, P.L. Show, Y. Ge, Y. Liu, R. Guo, J. Chen, Antibiotics: An overview on the environmental occurrence, toxicity, degradation, and removal methods, Bioengineered. 12 (2021) 7376–7416. https://doi.org/10.1080/21655979.2021.1974657.

[3] E.M. Cuerda-Correa, M.F. Alexandre-Franco, C. Fernández-González, Advanced oxidation processes for the removal of antibiotics from water. An overview, Water (Switzerland). 12 (2020). https://doi.org/10.3390/w12010102.

[4] A. Joss, S. Zabczynski, A. Göbel, B. Hoffmann, D. Löffler, C.S. McArdell, T.A. Ternes, A. Thomsen, H. Siegrist, Biological degradation of pharmaceuticals in municipal wastewater treatment: Proposing a classification scheme, Water Research. 40 (2006) 1686–1696. https://doi.org/10.1016/j.watres.2006.02.014.

[5] J.O. Ighalo, C.A. Igwegbe, C.O. Aniagor, S.N. Oba, A review of methods for the removal of penicillins from water, Journal of Water Process Engineering. 39 (2021) 101886. https://doi.org/10.1016/j.jwpe.2020.101886.

[6] X. Yang, K. Luo, Z. Pi, P. Shen, P. Zhou, L. He, X. Li, Q. Yang, Insight to the mechanism of tetracycline removal by ball-milled nanocomposite CeO2/Fe3O4/Biochar: Overlooked

degradation behavior, Separation and Purification Technology. 307 (2023) 122703. https://doi.org/10.1016/j.seppur.2022.122703.
[7] J. Wang, R. Zhuan, Degradation of antibiotics by advanced oxidation processes: An overview, Science of The Total Environment. 701 (2020) 135023. https://doi.org/10.1016/j.scitotenv.2019.135023.
[8] C.V. Rekhate, J.K. Srivastava, Recent advances in ozone-based advanced oxidation processes for treatment of wastewater- A review, Chemical Engineering Journal Advances. 3 (2020) 100031. https://doi.org/10.1016/j.ceja.2020.100031.
[9] M.Z. Akbari, Y. Xu, Z. Lu, L. Peng, Review of antibiotics treatment by advance oxidation processes, Environmental Advances. 5 (2021) 100111. https://doi.org/10.1016/j.envadv.2021.100111.
[10] J.J.L. Peñalver, C.V.G. Pacheco, M.S. Polo, J.R. Utrilla, Degradation of tetracyclines in different water matrices by advanced oxidation/reduction processes based on gamma radiation, Journal of Chemical Technology & Biotechnology. 88 (2013) 1096–1108. https://doi.org/10.1002/jctb.3946.
[11] Q. Dai, J. Wang, J. Chen, J. Chen, Ozonation catalyzed by cerium supported on activated carbon for the degradation of typical pharmaceutical wastewater, Separation and Purification Technology. 127 (2014) 112–120. https://doi.org/10.1016/j.seppur.2014.01.032.
[12] M. Francoeur, C. Yacou, C. Jean-Marius, Y. Chérémond, U. Jauregui-Haza, G. Sarra, Optimization of the synthesis of activated carbon prepared from *Sargassum (sp.)* and its use for tetracycline, penicillin, caffeine and methylene blue adsorption from contaminated water, Environmental Technology & Innovation. (2022) 102940. https://doi.org/10.1016/j.eti.2022.102940.
[13] A.G. Capodaglio, Critical perspective on advanced treatment processes for water and wastewater: AOPs, ARPs, and AORPs, Applied Sciences (Switzerland). 10 (2020). https://doi.org/10.3390/app10134549.
[14] Z.-Y. Lu, Y.-L. Ma, J.-T. Zhang, N.-S. Fan, B.-C. Huang, R.-C. Jin, A critical review of antibiotic removal strategies: Performance and mechanisms, Journal of Water Process Engineering. 38 (2020) 101681. https://doi.org/10.1016/j.jwpe.2020.101681.
[15] E. Issaka, J.N.-O. AMU-Darko, S. Yakubu, F.O. Fapohunda, N. Ali, M. Bilal, Advanced catalytic ozonation for degradation of pharmaceutical pollutants—A review, Chemosphere. 289 (2022) 133208. https://doi.org/10.1016/j.chemosphere.2021.133208.
[16] C. Mansas, J. Mendret, S. Brosillon, A. Ayral, Coupling catalytic ozonation and membrane separation: A review, Separation and Purification Technology. 236 (2020) 116221. https://doi.org/10.1016/j.seppur.2019.116221.
[17] R. Guillossou, J. Le Roux, S. Brosillon, R. Mailler, E. Vulliet, C. Morlay, F. Nauleau, V. Rocher, J. Gaspéri, Benefits of ozonation before activated carbon adsorption for the removal of organic micropollutants from wastewater effluents, Chemosphere. 245 (2020) 125530. https://doi.org/10.1016/j.chemosphere.2019.125530.
[18] P. Krasucka, B. Pan, Y. Sik Ok, D. Mohan, B. Sarkar, P. Oleszczuk, Engineered biochar – A sustainable solution for the removal of antibiotics from water, Chemical Engineering Journal. 405 (2021) 126926. https://doi.org/10.1016/j.cej.2020.126926.
[19] H. Vatankhah, S.M. Riley, C. Murray, O. Quiñones, K.X. Steirer, E.R.V. Dickenson, C. Bellona, Simultaneous ozone and granular activated carbon for advanced treatment of micropollutants in municipal wastewater effluent, Chemosphere. 234 (2019) 845–854. https://doi.org/10.1016/j.chemosphere.2019.06.082.
[20] F. Zietzschmann, R.-L. Mitchell, M. Jekel, Impacts of ozonation on the competition between organic micro-pollutants and effluent organic matter in powdered activated carbon adsorption, Water Research. 84 (2015) 153–160. https://doi.org/10.1016/j.watres.2015.07.031.
[21] J. Wang, H. Chen, Catalytic ozonation for water and wastewater treatment: Recent advances and perspective, Science of The Total Environment. 704 (2020) 135249. https://doi.org/10.1016/j.scitotenv.2019.135249.
[22] Y. Alvarez-Galvan, B. Minofar, Z. Futera, M. Francoeur, C. Jean-Marius, N. Brehm, C. Yacou, U.J. Jauregui-Haza, S. Gaspard, Adsorption of Hexavalent Chromium Using Activated Carbon Produced from *Sargassum ssp.*: Comparison between Lab Experiments and Molecular Dynamics Simulations, Molecules. 27 (2022) 6040. https://doi.org/10.3390/molecules27186040.
[23] M. Francoeur, A. Ferino-Pérez, C. Yacou, C. Jean-Marius, E. Emmanuel, Y. Chérémond, U. Jauregui-Haza, S. Gaspard, Activated carbon synthetized from *Sargassum (sp)* for adsorption of caffeine: Understanding the adsorption mechanism using molecular modeling, Journal of

Environmental Chemical Engineering. 9 (2021) 104795. https://doi.org/10.1016/j.jece.2020.104795.
[24] R. Ranguin, M. Delannoy, C. Yacou, C. Jean-Marius, C. Feidt, G. Rychen, S. Gaspard, Biochar and activated carbons preparation from invasive algae Sargassum spp. For Chlordecone availability reduction in contaminated soils, Journal of Environmental Chemical Engineering. 9 (2021). https://doi.org/10.1016/j.jece.2021.105280.
[25] X. Jin, C. Wu, L. Fu, X. Tian, P. Wang, Y. Zhou, J. Zuo, Development, dilemma and potential strategies for the application of nanocatalysts in wastewater catalytic ozonation: A review, Journal of Environmental Sciences. 124 (2023) 330–349. https://doi.org/10.1016/j.jes.2021.09.041.
[26] P. Loganathan, J. Kandasamy, S. Jamil, H. Ratnaweera, S. Vigneswaran, Ozonation/adsorption hybrid treatment system for improved removal of natural organic matter and organic micropollutants from water – A mini review and future perspectives, Chemosphere. 296 (2022) 133961. https://doi.org/10.1016/j.chemosphere.2022.133961.
[27] M.S. Elovitz, U. von Gunten, Hydroxyl Radical/Ozone Ratios During Ozonation Processes. I. The Rct Concept, Ozone: Science & Engineering. 21 (1999) 239–260. https://doi.org/10.1080/01919519908547239.
[28] J. Nawrocki, Catalytic ozonation in water: Controversies and questions. Discussion paper, Applied Catalysis B: Environmental. 142–143 (2013) 465–471. https://doi.org/10.1016/j.apcatb.2013.05.061.
[29] X. Zhu, Y. Liu, F. Qian, C. Zhou, S. Zhang, J. Chen, Preparation of magnetic porous carbon from waste hydrochar by simultaneous activation and magnetization for tetracycline removal, Bioresource Technology. 154 (2014) 209–214. https://doi.org/10.1016/j.biortech.2013.12.019.
[30] J. Zhou, F. Ma, H. Guo, Adsorption behavior of tetracycline from aqueous solution on ferroferric oxide nanoparticles assisted powdered activated carbon, Chemical Engineering Journal. 384 (2020) 123290. https://doi.org/10.1016/j.cej.2019.123290.
[31] K. Khaledi, G.M. Valdes Labrada, J. Soltan, B. Predicala, M. Nemati, Adsorptive removal of tetracycline and lincomycin from contaminated water using magnetized activated carbon, Journal of Environmental Chemical Engineering. 9 (2021) 105998. https://doi.org/10.1016/j.jece.2021.105998.
[32] E.K. Faulconer, N.V.H. von Reitzenstein, D.W. Mazyck, Optimization of magnetic powdered activated carbon for aqueous Hg(II) removal and magnetic recovery, J Hazard Mater. 199–200 (2012) 9–14. https://doi.org/10.1016/j.jhazmat.2011.10.023.
[33] J.-L. Hazemann, J.F. Bérar, A. Manceau, Rietveld Studies of the Aluminium-Iron Substitution in Synthetic Goethite, Materials Science Forum. 79–82 (1991) 821–826. https://doi.org/10.4028/www.scientific.net/MSF.79-82.821.
[34] M.M. AbdElhady, Preparation and Characterization of Chitosan/Zinc Oxide Nanoparticles for Imparting Antimicrobial and UV Protection to Cotton Fabric, International Journal of Carbohydrate Chemistry. 2012 (2012) e840591. https://doi.org/10.1155/2012/840591.
[35] A.K. Bordbar, A.A. Rastegari, R. Amiri, E. Ranjbakhsh, M. Abbasi, A.R. Khosropour, Characterization of modified magnetite nanoparticles for albumin immobilization, Biotechnol Res Int. 2014 (2014) 705068. https://doi.org/10.1155/2014/705068.
[36] U. Jans, J. Hoigné, Activated Carbon and Carbon Black Catalyzed Transformation of Aqueous Ozone into OH-Radicals, Ozone: Science & Engineering. 20 (1998) 67–90. https://doi.org/10.1080/01919519808547291.
[37] J.-S. Park, H. Choi, J. Cho, Kinetic decomposition of ozone and para-chlorobenzoic acid (pCBA) during catalytic ozonation, Water Research. 38 (2004) 2285–2292. https://doi.org/10.1016/j.watres.2004.01.040.
[38] H. Jung, H. Choi, Catalytic decomposition of ozone and para-Chlorobenzoic acid (pCBA) in the presence of nanosized ZnO, Applied Catalysis B: Environmental. 66 (2006) 288–294. https://doi.org/10.1016/j.apcatb.2006.03.009.
[39] Directives de qualité pour l'eau de boisson, 4e éd. intégrant le premier additif [Guidelines for drinking-water quality: 4th ed. incorporating first addendum], Genève : Organisation mondiale de la Santé, 2017. http://apps.who.int/iris.
[40] S. Psaltou, A. Karapatis, M. Mitrakas, A. Zouboulis, The role of metal ions on p-CBA degradation by catalytic ozonation, Journal of Environmental Chemical Engineering. 7 (2019) 103324. https://doi.org/10.1016/j.jece.2019.103324.
[41] K. Ikehata, N. Jodeiri Naghashkar, M. Gamal El-Din, Degradation of Aqueous Pharmaceuticals by Ozonation and Advanced Oxidation Processes: A Review, Ozone: Science & Engineering. 28 (2006) 353–414. https://doi.org/10.1080/01919510600985937.

[42] B. Kakavandi, N. Bahari, R. Rezaei Kalantary, E. Dehghani Fard, Enhanced sono-photocatalysis of tetracycline antibiotic using TiO_2 decorated on magnetic activated carbon (MAC@T) coupled with US and UV: A new hybrid system, Ultrasonics Sonochemistry. 55 (2019) 75–85. https://doi.org/10.1016/j.ultsonch.2019.02.026.
[43] J. Lu, J. Sun, X. Chen, S. Tian, D. Chen, C. He, Y. Xiong, Efficient mineralization of aqueous antibiotics by simultaneous catalytic ozonation and photocatalysis using $MgMnO_3$ as a bifunctional catalyst, Chemical Engineering Journal. 358 (2019) 48–57. https://doi.org/10.1016/j.cej.2018.08.198.
[44] R. Hekmatshoar, S. Khoramnejadian, A. Alahabadi, M.H. Saghi, Potential of ammonium chloride-activated carbon for decomposition of penicillin G by catalytic ozonation process (COP), International Journal of Environmental Science and Technology. (2021). https://doi.org/10.1007/s13762-021-03180-x.
[45] E.A. Agudelo, S.A. Cardona G., Advanced Oxidation Technology (Ozone-catalyzed by Powder Activated Carbon - Portland Cement) for the Degradation of the Meropenem Antibiotic, Ozone: Science & Engineering. 43 (2021) 88–105. https://doi.org/10.1080/01919512.2020.1796582.
[46] A.G. Gonçalves, J.J.M. Órfão, M.F.R. Pereira, Ozonation of erythromycin over carbon materials and ceria dispersed on carbon materials, Chemical Engineering Journal. 250 (2014) 366–376. https://doi.org/10.1016/j.cej.2014.04.012.
[47] M. Alameddine, A. Siraki, L. Tonoyan, M. Gamal El-Din, Treatment of a mixture of pharmaceuticals, herbicides and perfluorinated compounds by powdered activated carbon and ozone: Synergy, catalysis and insights into non-free OH contingent mechanisms, Science of The Total Environment. 777 (2021) 146138. https://doi.org/10.1016/j.scitotenv.2021.146138.